

Article

Comments about Rietveld Analysis and Tolerance Factor: Y Doped BaTiO₃

I. A. Lira-Hernández¹, F. R. Barrientos-Hernández¹, M. Pérez-Labra^{1,*},
A. M. García-Mercado² and J. A. Romero-Serrano³

¹ Academic Area of Earth Science and Materials, Universidad Autónoma del Estado de Hidalgo, AACTyM, Carretera Pachuca–Tulancingo km. 4.5, C.P. 42184, Mineral de la Reforma, Pachuca de Soto 42039, Hidalgo, México; ivanlira04@hotmail.com (I.A.L.-H.); frbh68@hotmail.com (F.R.B.-H.); romeroipn@hotmail.com (J.A.R.-S.)

² Mechanical Engineering Department, Technological Institute of Pachuca, Road México-Pachuca km. 87.5, Pachuca de Soto 42080, Hidalgo, México; canfed63@gmail.com

³ Metallurgy and Materials Department, ESIQIE-IPN. UPALM, Zacatenco, México 07738, D.F., México

* Correspondence: MIGUELABRA@hotmail.com; Tel.: +52-717-2000 (ext. 2297, 2280)

Abstract: The aim of this work is to compare two softwares (MAUD and TOPAS) based on the Rietveld algorithm and to test the concept of tolerance factor using the dissolution at high temperature of yttrium into BaTiO₃. In general, both softwares give up different values of the crystalline parameters however the trends are similar in most cases but the analysis of the strain and crystallite size in the BaTiO₃ crystals suggests that, in this particular case, MAUD offered results more consistent with the expected behavior. Using the crystalline parameters calculated by Rietveld, the tolerance factor values were obtained and these data suggest even better stability in the crystalline structure than that expected using theoretical parameters. Tolerance factor concept also indicates that Ti⁴⁺ should be preferred.

Keywords: A. Ceramics; A. Oxides; C. X-ray diffraction; D. Crystal structure; D. Microstructure

1. Introduction

The technique developed by Hugo Rietveld represented a qualitative leap in the analysis of X-Ray diffraction data. Several softwares have been commercially available through time. Nowadays, TOPAS and MAUD softwares are quite popular throughout the materials science researching literature. The method is, of course, basically the same but the computational efficiency and capabilities of the numerical algorithms that each software offer is the difference. The Rietveld method includes several parameters initially designed to qualify the reliability of the results in a simple manner but the experience has shown that the interpretation of such parameters are not that simple after all.

The output parameters of the Rietveld method include [1]:

$$R_{wp} = \left[\frac{\sum w_i (y_i(obs) - y_i(cal))^2}{\sum w_i (y_i(obs))^2} \right]^{1/2} \quad (1)$$

$$GOF = R_{wp} / R_{exp} \quad (2)$$

$$R_{exp} = [(N - P) / \sum w_i y_i^2]^{1/2} \quad (3)$$

Where:

$$w_i = 1 / y_i(obs)$$

$y_i(obs)$ = Observed (gross) intensity at the i th step,

$y_i(cal)$ = Calculated intensity at the i th step,

N = number of data points

P = number of parameters

The sum is carried out over all data points.

Observing equations 1 and 2, one could expect that the best fit occurs when $R_{wp} \rightarrow 0$ or when $GOF \rightarrow 1$, however the experience shows that is not exactly the case as it will be discussed later in this article.

One interesting case that can be used to test these softwares is the dissolution of yttrium into the BaTiO₃ crystalline lattice since yttrium can occupy both Ti⁴⁺ and Ba²⁺ cationic sites depending on several parameters such as the Ba/Ti ratio, the sintering temperature, etc. [2] However, regarding that the energy to create a Barium vacancy in the BaTiO₃ lattice has been reported as 5.94 eV whereas to form a Ti⁴⁺ vacancy is 7.56 eV it is expected that at high sintering temperatures the Yttrium ion can “choose” the crystalline site of equilibrium because at these temperatures there will be a high concentration of both cation vacancies whereas at low temperature only Ba vacancies would be available. A systematic study has been published elsewhere [3] where it has been supported that at 1500°C yttrium occupies the Ti site in the lattice. It is important to know which substitution is taking place because the electrical properties depend strongly on this matter.

Dissolution of Yttrium into BaTiO₃ is also a good case to test the concept of Tolerance Factor initially developed by Goldsmith [4]. In this concept it is assumed that the cubic structure is the most stable one for a perovskite type phase of a compound ABO₃, and it uses the ionic radii to measure how much the actual structure is deviated from the perfect cube. Such Tolerance Factor, t , is given as:

$$t = (A - O) / \sqrt{2}(B - O) \quad (4)$$

where (A-O) is the distance between the cation A and the oxygen and B-O is likewise the distance between the cation B and the oxygen. The factor $\sqrt{2}$ is added in order to that $t=1$ in the case of a perfect cubic structure. Any deviation from the unit would mean that the structure losses stability. The distance between the cations and the oxygen is quantified by the use of the ionic radii to become:

$$t = (rA - rO) / \sqrt{2}(rB - rO) \quad (5)$$

Where rA , rB , and rO are the ionic radii of A, B and O ions. To include the case of a solid solution, the mass law is used to recalculate the ionic radius of the ion which has been replaced by the solute ion. The ionic radii reported in literature are $rO = 0.140$ nm, $rBa = 0.135$ nm, $rTi = 0.068$ nm and $rY = 0.93$ nm [5]. Using these values plots of t as a function of Y³⁺ concentration can be drawn (Figure 1). As observed in Figure 1, the Tolerance factor concept predicts that the substitution of Ti⁴⁺ is more likely.

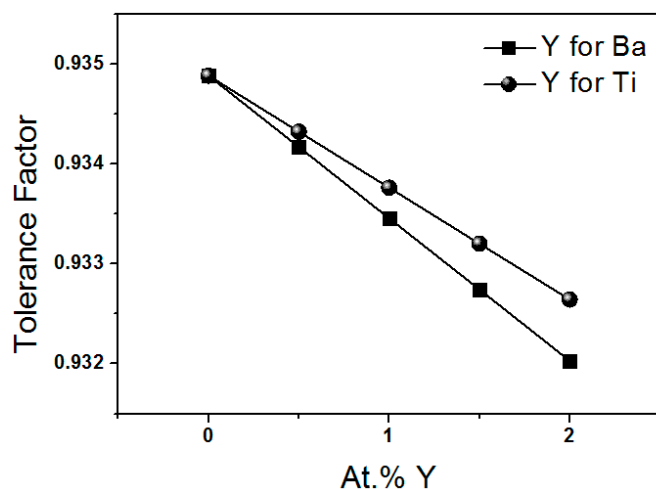


Figure 1. Tolerance factor for samples of Y doped-barium titanate

The t value of equations 4 and 5 can be compared to experimental results if it is observed that the distances between ions in equation 4 can be written as:

$$A - O = a/\sqrt{2} \quad (6)$$

$$B - O = c/2 \quad (7)$$

Where “a” and “c” are the lattice parameters of the tetragonal BaTiO₃ unit cell.

2. Experimental Section

The yttrium-doped BaTiO₃ ceramics were prepared using BaCO₃ Sigma 99% purity, TiO₂ Merck 99% purity and Y₂O₃ Aldrich 99.99% purity as precursors. The powders were mixed in a stoichiometric ratio according to Eq. (8) with the x values ranging from 0.005 to 0.02.



The powders were weighed and placed in a polyethylene container with de-ionized water and pellets of zirconia (ZrO₂) to homogenize the mixture for 24 hours by rotation. Excess of water was decanted and the powder was heated at 80°C for 18 hours to remove remaining water. The powder was recovered and sintered for 1 hour at 1500°C in a furnace Model (CARBOLITE RHF 17/3E (10°C/min)). The powders were characterized at room temperature using a Bruker D8 Focus Diffractometer at an increment of 0.04° and a 5 angle of incidence. A copper-K α ($\lambda=1.5418 \text{ \AA}$) target was used. Rietveld refinement was performed on all X-ray patterns using MAUD computer program and TOPAS Academic 4.1 software to determine the crystal structure and lattice parameters as a function of the doping level.

In the present work, we have adopted the Rietveld’s powder structure refinement analysis of X-ray powder diffraction step scan data of solid state reaction samples to obtain the refined structural and microstructural parameters (crystallite size and r.m.s. lattice strain). The Rietveld software MAUD is specially designed to refine simultaneously both the structural and microstructural parameters through a least-square method. The peak shape was assumed to be a pseudo-Voigt function with asymmetry. The background of each

pattern was fitted by a polynomial function of degree 4. The recently developed software MAUD, which is based on the Rietveld method combined with Fourier analysis, has been applied to analyze XRD data for alloys and ferroelectrics [6, 7]. TOPAS Academic 4.1 was also applied using the same assumptions than in the MAUD case.

3. Results and Discussion

Figure 2 shows the XRD patterns of yttrium doped BaTiO₃ samples. The peaks observed correspond to BaTiO₃ (ICDD PDF 05-0626) except for the small peak at 28.7° which correspond to orthotitanate Ba₆Ti₁₇O₄₀. Orthotitanate is formed from the reaction between TiO₂ and BaTiO₃. The XRD peaks are slightly displaced from the reflections reported for pure BaTiO₃ suggesting the formation of a solid solution. It has been proved that this shift is due to a distortion of the crystal structure (tetragonal) resulted from the yttrium substitution at titanium positions [3].

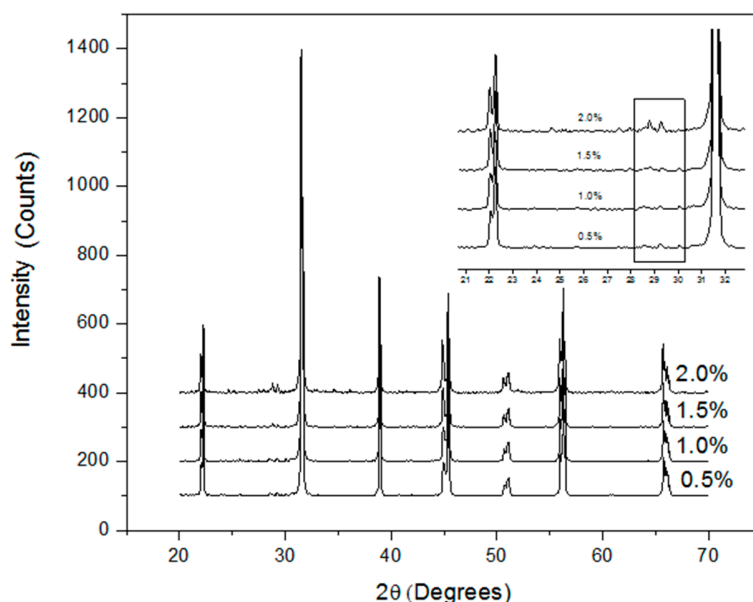


Figure 2. X-ray diffraction of the powders prepared at different doping levels

At room temperature, BaTiO₃ has a tetragonal structure characterized by lattice parameters “a” and “c”. Typical patterns resulted from Rietveld analyses for different concentrations of yttrium are shown in Figures 3 and 4, and compared to the experimental patterns. Rietveld analyses confirm that the main phase present in the samples after synthesis and sintering reactions is the tetragonal barium titanate. Patterns belonging to precursors were not observed.

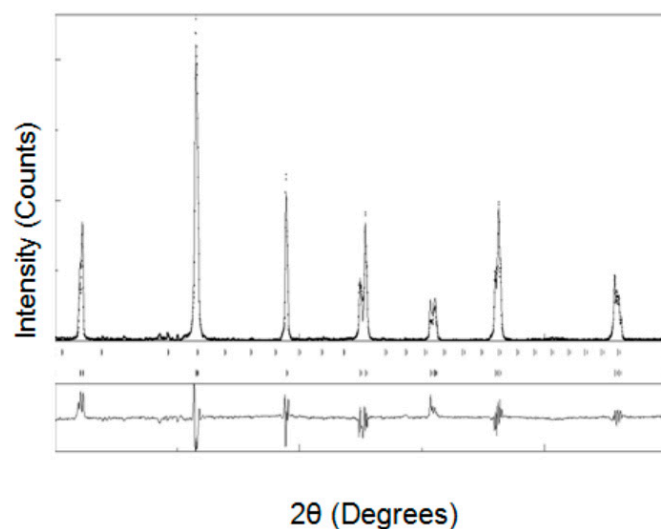


Figure 3. Rietveld refinement patterns of x-ray diffraction for x= 0.5 At Yttrium % MAUD

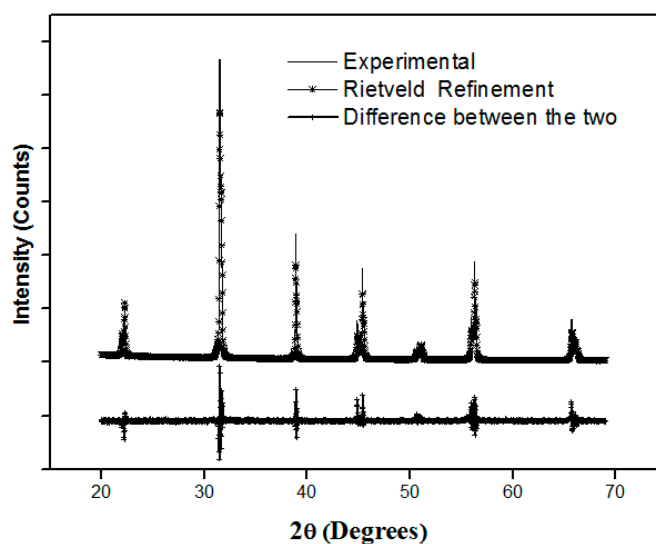


Figure 4. Rietveld refinement patterns of x-ray diffraction for x= 1. 5 At Yttrium % TOPAS

Initially, the positions of the peaks were corrected by successive refinements of zero-shift error. Considering the integrated intensity of the peaks as a function only of structural parameters, in the case of MAUD software the Marquardt least-squares procedures were adopted for minimization of the difference between the observed and the simulated powder diffraction patterns, and such minimization was carried out using the reliability index parameter [8].

TOPAS academic 4.1 was also used for Rietveld refinement in this work, a number of parameters were refined, including five background terms, five pseudo-Voigt profile function coefficients.

In both cases, refinement continued till convergence was reached with the value of the quality factor GOF around 1, which suggests a good refinement. In each case, all the output parameters as taken from the

softwares are shown in Tables 1 and 2 for comparison purposes. Parameters in Tables 1 and 2 other than GOF, Rwp and Rexp are not defined in this article because are not relevant for the discussion.

Table 1. Refined parameters of sample by rietveld refinement analyses with MAUD

Sample % at Y	Refined Parameters						
	Rexp	Rwp	Rp	Rwpb	Rpb	GOF	Sig.
0.5	9.3438	0.05690	0.02860	0.1298	0.0979	0.006	0.6089
1.0	6.8211	0.05069	0.02261	0.1493	0.0940	0.007	0.7432
1.5	5.6377	0.04244	0.01788	0.1607	0.0864	0.008	0.7527
2.0	4.8910	0.03068	0.01347	0.1145	0.0629	0.006	0.6273

Table 2. Refined parameters of sample by rietveld refinement analyses with TOPAS

Sample % at Y	Refined Parameters					
	Rexp	Rwp	Rp	Rwpb	Rpb	GOF
0.5	4.69122	6.943	5.589	12.847	9.760	1.480
1.0	4.24405	6.243	5.004	12.675	9.469	1.471
1.5	5.39427	6.964	5.466	11.662	8.771	1.291
2.0	5.65874	8.092	6.226	12.827	9.542	1.430

Although the algorithm is basically the same (Rietveld algorithm), tutorials of MAUD and TOPAS software emphasize different parameters to evaluate the goodness of fitting. MAUD tutorial points out the parameters Rexp and sig as the important parameters. According to this tutorial, $Rexp < 15.0$ and $sig < 2.0$, suggest good fitting, and, as observed in Table 1 these conditions are fulfilled in our results. M.R. Panigrahi et al. argued a good fitting with values of $Rwp = 0.768$ and $GOF = 0.24$. According to S. Bid et al. [9], in our case, values of Rwp and sig suggest that the refinement is good but the values of GOF are out of range.

Regarding TOPAS software, a GOF factor greater than 1.5 is a strong indication of an inadequate model or false minimum. A value of the GOF factor less than 1.0, however, is an indication not of an extremely high quality refinement as could be expected but of a model that contains more parameters than can be justified by the quality of the data [10]. Values of GOF between 1.09 and 1.28 would confirm a good refinement [9]. According to Pourghahramani et al. [11] the goodness factor values for our experiments imply satisfactory fit to the measured data.

In Figure 5 the lattice parameters as a function of Y^{3+} concentration are presented. As observed, Figure 5 suggests that, in general, the values of lattice parameters increase when the concentration of Y^{3+} increases. However, this trend is more evident for "c" parameter showing the asymmetry of the atomic bonds. In an ionic crystal, such as $BaTiO_3$, electron orbitals are approximately spherical due to electron exchange between anions and cations. However, because of the difference in valence between Y^{3+} and Ti^{4+} the inert atom configuration cannot be attained and some asymmetry could be expected in the Y^{3+} ion. The P4mmm tetragonal structure is maintained in all Y^{3+} concentrations.

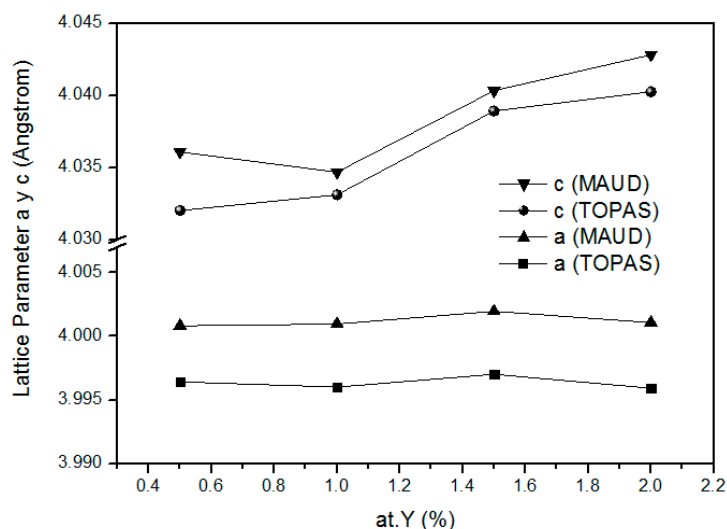


Figure 5. Lattice parameters of a tetragonal unit cell (ICSD-05 0626) as a function of Y^{3+} concentration

The unit cell volume increases when the Y^{3+} increases (Figure 6) which can be explained on the difference in ionic sizes between Y^{3+} (0.93 nm) and Ti^{4+} (0.068 nm). It must be notice that the deformation of the unit cell produced by the solid solution is not only due to the substitution of one small ion for other which is bigger, but also the production of oxygen vacancies is involved [3]. In both Figures, it seems that there is a systematic shift between the output values from TOPAS and MAUD softwares and there is no way to decide which one is more accurate. In the case of the unit cell volume, the difference is almost constant and around 0.2 \AA^3 .

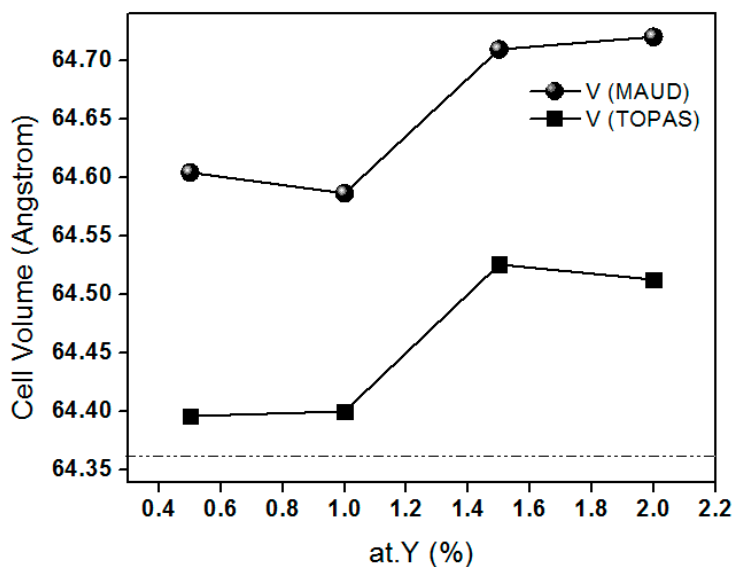


Figure 6. Unit cell volume as a function of Y^{3+} concentration. The dotted line is the unit cell volume according the file ICDS-5 0626

Crystallite size and microstrain as a function of Y^{3+} concentration is presented in Figure 7 and 8 respectively. The values of crystallite size ranging from 100 to 400 nm are quite reasonable. The microstrain values observed in Figure 8 are very small which is expected due to the fragile character of a

ceramic (BaTiO_3). To assess whether the behaviors shown in Figures 7 and 8 are the expected, the graph of grain size as a function of Y^{3+} concentration is necessary and it is presented in Figure 9.

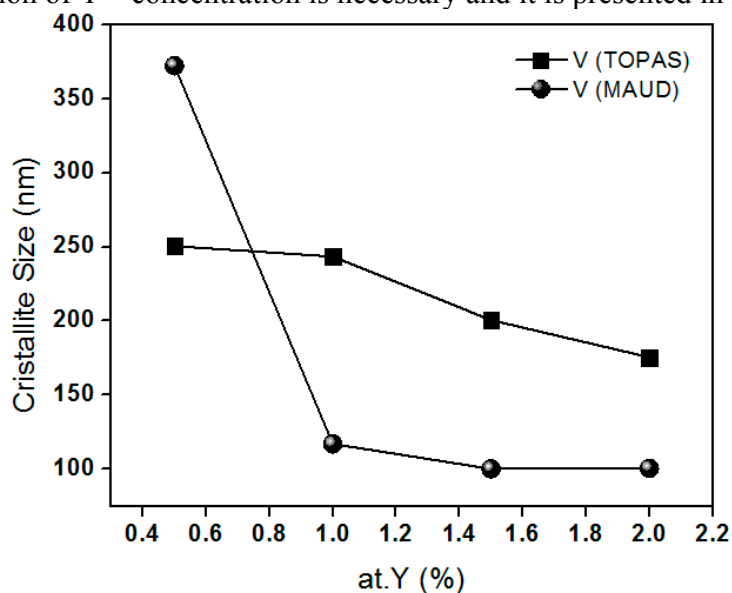


Figure 7. Crystallite size as a function of Y concentration

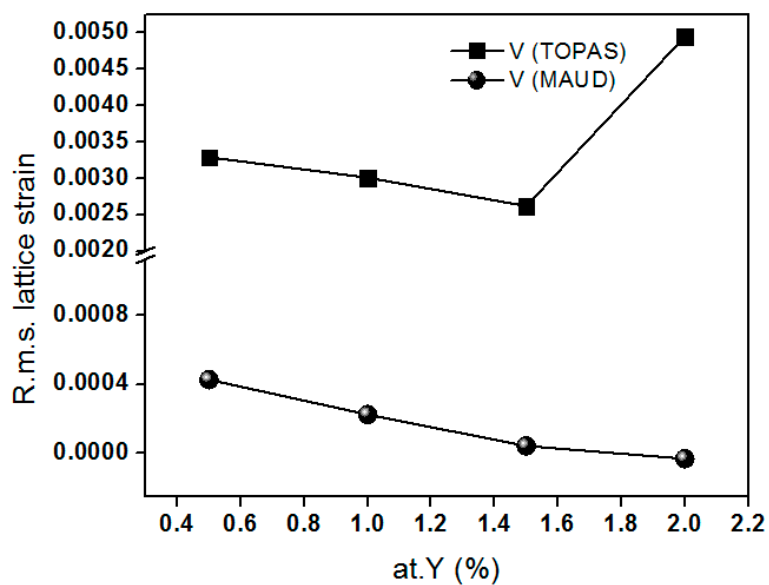


Figure 8. R.m.s lattice strain as a function of Y concentration

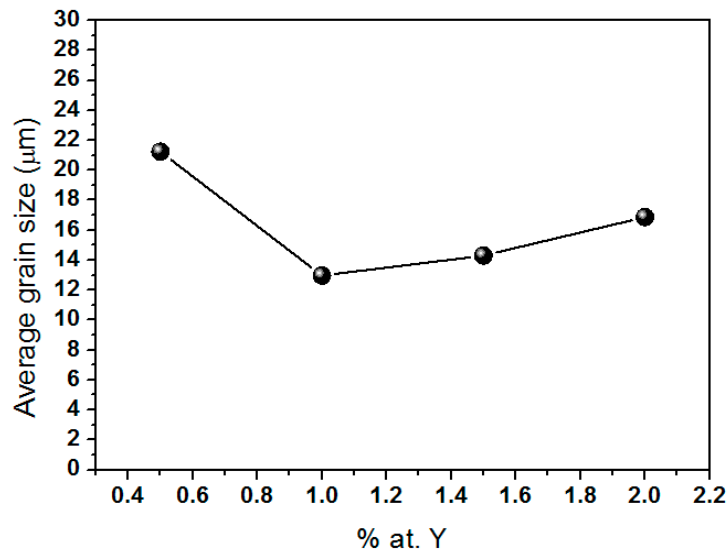


Figure 9. Average grain size as function of Y^{3+} concentration

It is commonly seen that the higher the dopant concentration the smaller the grain size, this behavior is due to two main reasons: first, when a solute is added to the crystalline lattice, some deformation occurs which makes difficult the growing of a perfect lattice during sintering and eventually a grain boundary is built up. Second, when the dopant concentration is relatively high, the dissolution becomes harder and particles of the dopant precursor (in this case Y_2O_3) play the role of nucleation points. In Figure 9, a decreasing from 22 to 12 microns in the grain size is observed at low Y^{3+} concentrations and then the grain size remains without big changes although a mild increasing is observed. If the grain size is decreasing it is expected that the crystallite size, that is, the coherent regions inside the grains, also decreases as shown in Figure 7. The strong reduction in the grain size observed in Figure 9 in the region 0.4 to 1 at % Y, corresponds to a strong reduction in the crystallite size for the MAUD case in Figure 7 but this strong reduction is not observed for the TOPAS case.

The sintering process tends to build up residual strain inside the grains as the grain growing is taking place and also during the cooling stage due to thermal contraction. However, because the material is fragile, high amounts of deformation are not possible because fracture occurs at small levels of deformation. When fracture occurs the residual strains are released and the fracture plane evolves eventually into a grain boundary. Therefore, it is expected that the strain in the lattice decreases when the grain size decreases just as observed in Figures 8 and 9. In Figure 8 the TOPAS software shows an increase in the microstrain at high Y^{3+} concentrations which is hard to believe.

The lattice parameters calculated by MAUD and TOPAS softwares can be used to calculate the Tolerance Factor using the expressions 6 and 7. In this way it is possible to test the Tolerance Factor concept. However, the concept of ionic size assumes that ions are hard balls and therefore these sizes cannot be compared just as reported in literature. In order to compare the theoretical values with Rietveld calculations, the theoretical values plotted in Figure 1 were shift up to coincide to the experimental values for pure $BaTiO_3$ by adding a constant value. The comparison is presented in Figure 10. As observed, experimental t values are higher than theoretical ones suggesting more stability than expected. Since the Rietveld curves are not linear, least square fitting was carried out and the slopes are presented in Table 3.

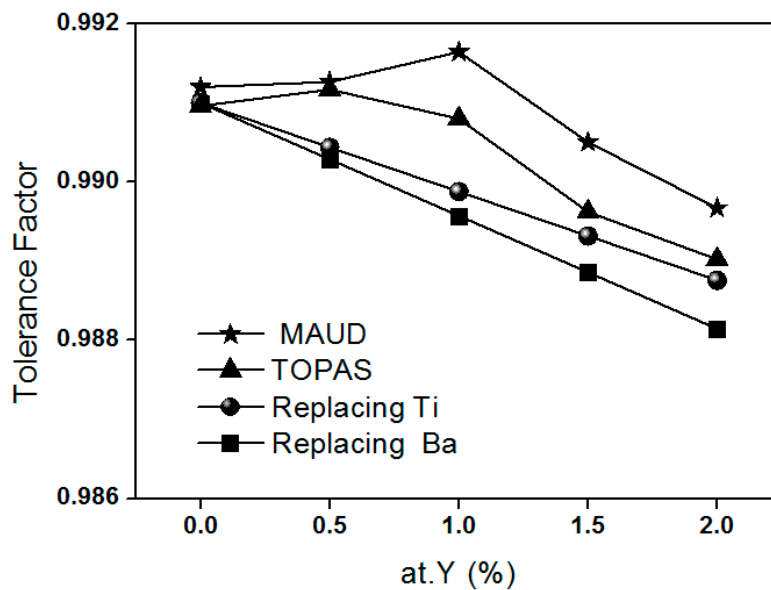


Figure 10. Tolerance factor as a function of Y concentration for different cases

Table 3. Slopes of the curves shown in figure 10 after least square fitting

Curve	Slope ($\times 10^{-5}$)
MAUD	-76
TOPAS	-100
Replacing Ti	-110
Replacing Ba	-143

As observed, slopes of Rietveld curves have a closer value to the slope for the line corresponding to the Ti substitution, suggesting that Ti substitution is the most likely which, indeed, has been experimentally well supported elsewhere [3].

4. Conclusions

Comparison between the MAUD and TOPAS softwares, presented in this work, suggests that can be very important the optimization of the numeric routines since, although basic parameters (in our case the lattice parameters) could be basically right, some others can be far to be precise. On other hand the tolerance factor concept showed to be a solid concept in spite of its simplicity and it suggests that the actual crystalline structure is more thermodynamically stable than predicted

Acknowledgements: The authors gratefully acknowledge to PRODEP Mexico, for the financial support for this work.

Author Contributions: I. A. Lira-Hernández and José-Antonio Romero-Serrano analyzed the data, Miguel Pérez-Labra, F. R. Barrientos-Hernández and, A. M. García-Mercado performed the experiments; all authors approved this manuscript.

Conflicts of Interest: The authors declare no conflict of interest.

References

- [1] E. Prince, Mathematical aspects of Rietveld refinement, in *The Rietveld Method*, edited by R. A. Young, Oxford University Press, Great Britain, **1995**.
- [2] D.M. Smyth, *The Defect Chemistry of Metal Oxides*, Oxford University Press, New York, **2000**.
- [3] M. Paredes, I.A. Lira, C. Gomez, F. Espino, Compensation mechanisms at high temperature in Y-doped BaTiO₃. *Physica B: Condensed Matter*. **2013**, 410, 157-161. doi.org/10.1016/j.physb.2012.11.001
- [4] A. Rüdiger, Defect structure of oxide ferroelectrics—valence state, site of incorporation, mechanisms of charge compensation and internal bias field. *Journal of Electroceramics*. 2007, 19, 11-23. doi:10.1007/s10832-007-9068-8.
- [5] M.T. Buscaglia, V. Buscaglia, M. Viviani, P. Nanni, M. Hanuskova, *Journal of the European Ceramic Society*. Influence of foreign ions on the crystal structure of BaTiO₃. **2000**, 20, 1997-2007. doi.org/10.1016/S0955-2219(00)00076-5.
- [6] P. Sahu, S.K. Pradhan, X-ray diffraction studies of the decomposition and microstructural characterization of cold-worked powders of Cu–15Ni–Sn alloys by Rietveld analysis. *Journal of Alloys and Compounds*. **2004**, 377, 103-116. doi.org/10.1016/j.jallcom.2003.10.019.
- [7] L. Cont, D. Chateigner, L. Lutterotti, J. Ricote, M. L. Calzada, and J. Mendiola, Combined X-ray Texture-Structure-Microstructure Analysis Applied to Ferroelectric Ultrastructures: A Case Study on Pb_{0.76}Ca_{0.24}TiO₃. *Ferroelectrics*. **2002**, 267, 323-328. doi.org/10.1080/00150190211032.
- [8] M.R. Panigrahi, S. Panigrahi, Rietveld analysis of single phase Ba_{0.99}Dy_{0.01}TiO₃ ceramic. *Physica B: Condensed Matter*. **2010**, 405, 3986-3990. doi.org/10.1016/j.physb.2010.06.043.
- [9] S. Bid, S.K. Pradhan, Preparation of zinc ferrite by high-energy ball-milling and microstructure characterization by Rietveld's analysis. *Materials Chemistry and Physics*. **2003**, 82, 27-37. doi.org/10.1016/S0254-0584(03)00169-X.
- [10] R.A. Young, D.B. Wiles, Profile shape functions in Rietveld refinements. *Journal of Applied Crystallography*. **1993**, 15, 430-434. doi.org/10.1107/S002188988201231X.
- [11] P. Pourghhramani, E. Altin, M. Rao, W. Peukert E. Forssberg, Microstructural characterization of hematite during wet and dry millings using Rietveld and XRD line profile analyses. *Powder Technology*. **2008**, 186, 9-21. doi.org/10.1016/j.powtec.2007.10.027.



© 2016 by the authors; licensee *Preprints*, Basel, Switzerland. This article is an open access article distributed under the terms and conditions of the Creative Commons by Attribution (CC-BY) license (<http://creativecommons.org/licenses/by/4.0/>).